

Combined Chemoradionuclide Therapy Using Poly(ϵ -caprolactone-b-ethylene oxide) Micelles as the Delivery Vehicle

Liu, Huanhuan; Nadar, Robin A.; Fauzia, Retna Putri; Laan, Adrianus C.; Wang, Runze; van Cooten, Quenteijn; Carroll, Elizabeth C.M.; Eelkema, Rienk; Denkova, Antonia G.; More Authors

DOI

[10.1002/adtp.202200224](https://doi.org/10.1002/adtp.202200224)

Publication date

2023

Document Version

Final published version

Published in

Advanced Therapeutics

Citation (APA)

Liu, H., Nadar, R. A., Fauzia, R. P., Laan, A. C., Wang, R., van Cooten, Q., Carroll, E. C. M., Eelkema, R., Denkova, A. G., & More Authors (2023). Combined Chemoradionuclide Therapy Using Poly(ϵ -caprolactone-b-ethylene oxide) Micelles as the Delivery Vehicle. *Advanced Therapeutics*, 6(5), Article 2200224. <https://doi.org/10.1002/adtp.202200224>

Important note

To cite this publication, please use the final published version (if applicable).
Please check the document version above.

Copyright

Other than for strictly personal use, it is not permitted to download, forward or distribute the text or part of it, without the consent of the author(s) and/or copyright holder(s), unless the work is under an open content license such as Creative Commons.

Takedown policy

Please contact us and provide details if you believe this document breaches copyrights.
We will remove access to the work immediately and investigate your claim.

Combined Chemoradionuclide Therapy Using Poly(ϵ -caprolactone-b-ethylene oxide) Micelles as the Delivery Vehicle

Huanhuan Liu, Robin A. Nadar, Retna Putri Fauzia, Adrianus C. Laan, Britt Doeswijk, Runze Wang, Astrid van de Meer, Quenteijn van Cooten, Elizabeth C. M. Carroll, Rienk Eelkema,* and Antonia G. Denkova*

Combination of therapies is a common strategy in cancer treatment. Such combined therapies only have merit provided that there is superior therapeutic outcome with fewer side effects, compared to single therapies. Here, this work explores the possibility to combine chemotherapy with radionuclide therapy using polymeric micelles as a delivery vehicle. For this purpose, this work prepares poly(ϵ -caprolactone-b-ethylene oxide) (PCL-PEO) micelles and load them simultaneously with paclitaxel (PTX) and $^{177}\text{Lu(III)}$. This work chooses a 3D tumor spheroid composed of glioblastoma cells (U87) to evaluate the combined treatment. The diffusion of the micelles in the spheroid is investigated by confocal laser scanning microscopy (CLSM) and light-sheet fluorescence microscopy (LSFM). The results show that the micelles are able to penetrate deep into the spheroid within 24 h of incubation and mainly accumulated around or in the lysosomes once in the cell. Subsequently, this work evaluates the cell killing efficiency of the single treatments (PTX or $^{177}\text{Lu(III)}$) versus combined treatment (PTX + $^{177}\text{Lu(III)}$) by measuring the growth of the spheroids as well as by performing a cell-viability assay. The results indicate that the combined therapy achieves a superior therapeutic outcome with better cell growth inhibition and cell killing efficiency compared to the single treatments.

as well as adjuvant chemotherapy have been shown in many cases to result in better treatment efficacy.^[1] Possible reasons for the enhanced therapeutic outcome of radiochemotherapy are the synergistic excessive oxidative loading at the tumor sites,^[2] the arrest of tumor cells in the G2/M phase of the cell cycle by chemotherapeutics making them more sensitive to radiation,^[3] improved uptake of chemotherapeutics as result of radiation exposure,^[4] and reduced ability of tumor cells to repair deoxyribonucleic acid (DNA) damage caused by radiation.^[5] Although the exact mechanism behind radiochemotherapy is still not fully understood, this combined therapy has already become the standard treatment for certain cancer types, e.g. non-small cell lung cancer.^[6]

In clinical practice, radiochemotherapy is usually carried out by simply applying external beam therapy with chemotherapy according to different operation protocols, for instance by irradiating the patient shortly after chemotherapy.^[7,8] One of the main issues of this combined therapy is the severity


of the side effects. For instance, in the case of esophagus cancer, the patients treated with radiochemotherapy indeed showed higher survival than the groups treated with radiotherapy alone,

1. Introduction

Currently, the three main approaches for cancer treatment are surgery, radiotherapy, and chemotherapy. Combined therapies

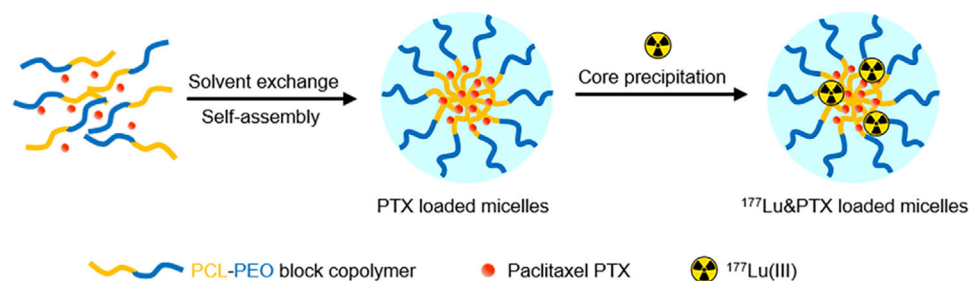
H. Liu, R. A. Nadar, R. P. Fauzia, A. C. Laan, B. Doeswijk, R. Wang, A. van de Meer, Q. van Cooten, A. G. Denkova
Department of Radiation Science and Technology
Delft University of Technology
Mekelweg 15, Delft 2629 JB, The Netherlands
E-mail: a.g.denkova@tudelft.nl

R. A. Nadar
Department of Radiation Oncology
Erasmus MC Cancer Institute
Rotterdam 3015GD, The Netherlands
R. P. Fauzia
Department of Biotechnology
Delft University of Technology
van der Maasweg 9, Delft 2629 HZ, The Netherlands
E. C. M. Carroll
Department of Imaging Physics
Delft University of Technology
Lorentzweg 1, Delft 2628 CJ, The Netherlands
R. Eelkema
Department of Chemical Engineering
Delft University of Technology
van der Maasweg 9, Delft 2629 HZ, The Netherlands
E-mail: R.Eelkema@tudelft.nl

 The ORCID identification number(s) for the author(s) of this article can be found under <https://doi.org/10.1002/adtp.202200224>

© 2023 The Authors. *Advanced Therapeutics* published by Wiley-VCH GmbH. This is an open access article under the terms of the Creative Commons Attribution-NonCommercial License, which permits use, distribution and reproduction in any medium, provided the original work is properly cited and is not used for commercial purposes.

DOI: 10.1002/adtp.202200224



Scheme 1. The process of making $^{177}\text{Lu(III)}$ and paclitaxel (PTX) co-loaded micelles

but they also experienced considerably more complications due to the toxicity of the drugs.^[9] The occurrence of additional adverse reactions is also one of the reasons that internal radionuclide therapy is hardly ever combined with chemotherapy, although studies suggest that such a combination would lead to much better treatment outcome.^[10–13] Clearly, if the side effects of combining these therapies are reduced, radiochemotherapy will become a more appealing treatment option.

One way to diminish side effects of chemotherapeutic drugs is to use nanocarriers since they can actively or passively deliver the therapeutic reagent to tumor tissue preventing the free drug from accumulating in healthy organs.^[14,15] Although some nanocarriers have even been translated to the clinic, their application in combined therapies have only been preclinically tested and most of the examples use external beam radiation. For instance, Werner et al. applied simple micelles composed of poly(ethylene glycol)-block-poly(D,L-lactide) (PEG-PDLLA) for the delivery of paclitaxel (PTX) in combination with external radiotherapy showing the radiosensitization properties of the drug and the ability of the nanocarrier to reduce drug toxicity to the lungs.^[16] An interesting approach to reduce side effects was proposed by Gao et al. who developed Se based polymer nanoparticles encapsulating doxorubicin (DOX). The selenium introduced in the nanoparticles helped to release DOX when exposed to an external gamma source, resulting in much more efficient cell killing.^[17] Still, only a few reports can be found in the literature in which nanocarriers were used for combined radionuclide therapy and chemotherapy. One nice example is the study by Wang et al. who applied lipid-polymer nanocarriers and DOX radiolabeled with the therapeutic isotope ^{90}Y , which is commonly applied in radionuclide therapy.^[18] The results showed better cell killing efficacy of the combined treatment which was enhanced by applying targeting vectors. Another interesting work concerns the thermosensitive polymeric hydrogels designed by Huang et al. in which both DOX and the therapeutic isotope ^{131}I were encapsulated.^[19] In vivo evaluation revealed much better tumor control in the mice treated with the combined therapy when compared to DOX or ^{131}I on their own. Additionally, no damage to healthy organs was observed. Even though these examples are promising, they require either elaborate preparation of the nanocarriers or complex radiolabeling procedures, which both hamper eventual translation to the clinic.

In this paper, we propose applying simple polymeric micelles composed of poly(ϵ -caprolactone-*b*-ethylene oxide) (PCL-PEO) which are degradable, easy to prepare, and can be simultaneously

loaded with chemotherapeutic drugs and radionuclides in a single step as shown in **Scheme 1**.^[14] We selected paclitaxel (PTX) as the chemotherapeutic drug and $^{177}\text{Lu(III)}$ as the therapeutic radionuclide. $^{177}\text{Lu(III)}$ is currently one of the most applied radionuclides in targeted radionuclide therapy. To determine the potential of this formulation we investigated the combined therapeutic effects using 3D tumor models. Moreover, we also studied the uptake of the micelles in 2D cell cultures and their diffusion in 3D tumor models.

2. Experimental Section

2.1. Materials

Poly(ϵ -caprolactone-*b*-ethylene oxide) block copolymers PCL-PEO (2800-2000), PCL-PEO (6500-5500) were bought from Polymer Source (Quebec, Canada). PTX, 4-(2-hydroxyethyl)-1-piperazineethanesulfonic acid (HEPES), chloroform, Sephadex G-25 resins, fluorescein isothiocyanate (FITC) and paraformaldehyde (PFA) were bought from Sigma Aldrich (Zwijndrecht, the Netherlands). ^{111}In and ^{177}Lu (in 0.01 M Hydrochloric acid (HCl) solution, the specific activity was 15.5 and 0.5 GBq μg^{-1} for ^{111}In and ^{177}Lu , respectively) were kind gifts of Erasmus Medical Centre (Rotterdam, the Netherlands). The Dulbecco's modified eagle medium (DMEM) culture medium, fetal bovine serum (FBS), penicillin-streptomycin solution 100 \times , PBS, and trypsin-ethylenediaminetetraacetic acid 1 \times (Trypsin-EDTA) were purchased from Biowest (Amsterdam, the Netherlands). Human U87 glioblastoma cells were obtained from VU Medical Centre Amsterdam (Amsterdam, the Netherlands). The CellTiter-Glo 3D Cell Viability Assay reagent was obtained from Promega (Leiden, the Netherlands). Plasma membrane marker (MemBrite Fix 568/580, Biotium) was used to label the membrane of the spheroids for imaging purposes. NucBlue Fixed cell stain ReadyProbes reagent (DAPI) and LysoTracker Red DND-99 were purchased from Thermo Fisher.

2.2. Synthesis

2.2.1. Preparation of PCL-PEO Micelles and PTX-Loaded Micelles

The PCL-PEO micelles were prepared by the solvent evaporation method described in our previous work.^[20] The drug-loaded micelles were also prepared using the same method. Typically, the

polymer stock solutions and PTX solutions were prepared by dissolving the polymer/PTX powder in chloroform. Sonication was applied to speed up the dissolving process until transparent solution was achieved. Then, 0.1 mL of the polymer stock solution (200 mg mL⁻¹, in chloroform) was mixed with 0.1 mL of the PTX solution (with different PTX concentrations ranging from 5, 7.5, 10, and 20 mg mL⁻¹) under sonication. The mixture was added dropwise to 2.3 mL of MQ water using a pipette. In this process, the tip of the pipette was kept below the water level. After the addition of the mixture, a turbid solution was achieved, which stirred overnight to evaporate the chloroform and induce micellization. Syringe filters with 220 nm cut-off were applied to remove large structures in the micelles and PTX-loaded micelles. Subsequently, the unencapsulated drugs were removed by size exclusion chromatography (SEC) which further diluted the polymer concentration to ≈2.2 mg mL⁻¹. Milli-Q (MQ) water was used as the eluent for SEC. Every 1 mL of eluent was collected as one fraction. The PTX-loaded micelles appeared in the 9th to 12th fractions, therefore 4 mL of samples were eventually collected. After the above process, the polymer concentration for the empty micelles sample and PTX-loaded micelles sample was around 8.7 and 2.2 mg mL⁻¹ (assuming that the polymer loss during the filtration was negligible).

2.2.2. Synthesis of ¹¹¹In(III) Radiolabeled Micelles

First, a centrifugation filter was used to concentrate the micelle sample which yielded a final solution with polymer concentration of 17.4 mg mL⁻¹. An amount of 2 mL of the sample was transferred to a 4 mL centrifugation filter with 10 kDa cut-off and centrifuged at 4000 rpm for 30 min. Then 2 mL of MQ water was added to wash the residual samples, followed by centrifugation for additional 30 min. The left samples were collected and the volume was adjusted to 1 mL. Then, the concentrated micelle solution was mixed with HEPES buffer (20 × 10⁻³ M, pH 7.4) in a volume ratio of 1:1. To radiolabel the micelles with ¹¹¹In(III), 15 MBq of ¹¹¹In was added to 0.4 mL of the micelle solution (8.7 mg mL⁻¹, in 10 × 10⁻³ M HEPES) and stirred for 0.5 h. The obtained samples were passed through a SEC to remove the free ¹¹¹In(III) species that were not encapsulated, during which HEPES buffer (10 × 10⁻³ M, pH = 7.4) was used as the eluent. Similarly, the radiolabeled micelles eluted in the 9th to 12th fractions, therefore 4 mL of samples were eventually collected and the final concentration of the samples was 0.87 mg mL⁻¹.

The centrifugation filters were also been applied in later experiments to concentrate or replace the solvent of the sample.

2.2.3. Synthesis of FITC-Labeled Micelles

The FITC-loaded PCL micelles were prepared by adding 0.1 mL of FITC stock solution (5 mg mL⁻¹ in ethanol) right after the addition of polymer stock solution into water. After being stirred overnight, 1 mL of the obtained mixture was passed through SEC to remove the unencapsulated FITC. MQ water was used as the eluent, and five fractions from 8th to 12th were collected as the

FITC-labeled micelles (5 mL, polymer concentration: 1.74 mg mL⁻¹).

2.2.4. Synthesis of ¹⁷⁷Lu(III) Radiolabeled Micelles

To make the ¹⁷⁷Lu(III) loaded micelles, 20 MBq of ¹⁷⁷Lu(III) was added to 1 mL of micelles solution (8.7 mg mL⁻¹, in HEPES) and stirred for half an hour. SEC was utilized again to separate the free ¹⁷⁷Lu(III) species. An amount of 1 mL of the samples was passed through the SEC column and eluted with HEPES. The same fractions were collected as in the ¹¹¹In experiments giving four fractions as the ¹⁷⁷Lu(III) radiolabeled samples which means that the polymer concentration of these samples was approximately 2.2 mg mL⁻¹.

2.2.5. Synthesis of ¹⁷⁷Lu@PTX Co-Loaded Micelles

To prepare the co-loaded micelles, the PTX-loaded micelles were first prepared with the PTX/polymer mass ratio of 0.05:20 (mg). Then, a 220 nm cut-off filter was applied to remove any large particulates present in the solution, and SEC was used to remove the unencapsulated PTX. Four milliliters of PTX-loaded micelles were collected after the SEC, which was concentrated to 1 mL and mixed with HEPES buffer with volume ratio of 1:1. Next, 10 MBq of ¹⁷⁷Lu(III) was added to 1 mL of PTX-loaded micelles (in HEPES buffer, polymer concentration was 4.3 mg mL⁻¹), followed by being stirred for 1 h. Then SEC columns were used to remove the unencapsulated ¹⁷⁷Lu(III), and 9th – 12th fractions of the eluents were collected as the ¹⁷⁷Lu@PTX co-loaded micelles for further use.

3. Characterization

3.1. Instruments

A dynamic light scattering (DLS) instrument consisting of a JDS uniphase 633 nm 35 mW laser, an ALV sp 125 s/w 93 goniometer, a fiber detector, and a Perkin Elmer photo counter were employed to determine the size distributions of the obtained micelles. A cryogenic electron microscope (Cryo-EM, Jeol JEM 1400) was used to image the morphology of the micelles. A high-performance liquid chromatography (HPLC, Agilent 1260) coupled to a UV detector set at 227 nm was applied to determine the drug concentration. A C18 column (15 cm × 4.6 mm) was applied. An amount of 50 μL was set as the injection volume. The mobile phase was a mixture of acetonitrile and aqueous formic acid solution (10 × 10⁻³ M) having a volume ratio of 45:55, respectively. An automatic gamma counter (Wallac WIZARD² 2480, Perkin Elmer Technologies) was used to determine the radiolabeling efficiency. A 12MP camera connected to the binocular microscope using automated imaging software (SampleScan) was utilized to record the images of the tumor spheroids. A Cary Eclipse Fluorescence Spectrophotometer (Agilent technologies) was utilized to measure the luminescence by choosing Bio/chemiluminescence data mode with the emission wavelength 600 nm, emission slit 20 nm, open emission filter, and selected gate time of 50 ms.

3.2. Characterization

3.2.1. Size Distribution

Size distribution of the as-prepared micelles were determined by DLS. For the DLS measurement, 0.1 mL of the obtained PCL-PEO micelles was added to a silica tubes containing 1.9 mL of MQ water, resulting a diluted micelles solution with a polymer concentration of 0.41 mg mL⁻¹. The tube containing micelles was placed in the sample holder with a fixed operation temperature of 22 ± 1 °C and a fixed scattered light angle of 90°.

3.2.2. Drug Loading Efficiency

THF was added to the micelle solutions under a volume ratio of 1:1 and left until a homogeneous solution had formed for disintegrating the drug-loaded micelles. Subsequently the HPLC setup was used to detect the PTX concentration in each sample.

The loading efficiency (LE) was calculated as follows:

$$\text{LE (\%)} \text{ of drugs (PTX)} = \frac{\text{The amount of drugs in final samples}}{\text{The initial drug amount}} \times 100\% \quad (1)$$

3.3. Cell studies

3.3.1. Cell line

Human U87 glioblastoma cells were used for the in vitro experiments. The cells were maintained in (DMEM) high glucose culture medium supplemented with 10% fetal bovine serum (FBS) and 1% penicillin/streptomycin under humidified normoxic (95% air, 5% CO₂) at 37 °C. For preparation of 3D cell models, 2000 cells (suspended in 200 µL cell culture medium) were seeded in each well in a U shape 96-well plate and incubated for 5 days before use. For preparation of the 2D cell model, 1 × 10⁵ cells (suspended in 250 µL cell culture medium) were seeded in a dish specific for confocal imaging and incubated overnight before use.

3.3.2. Cell Uptake

The cell uptake was evaluated by using ¹¹¹In(III) radiolabeled micelles. Centrifuge filter tubes were applied to replace the solvent (HEPES) with phosphate buffered saline (PBS; pH 7.4) before feeding the micelles to the cells. Then, 20 µL of ¹¹¹In(III) labeled micelles were added to each tumor spheroid to achieve a final micelle concentration of 0.079 mg mL⁻¹. The spheroids were harvested and washed with 4 mL of PBS (4 × 1 mL) at certain time points (5 h, 1 d, 2 d, 3 d). The final activity in each spheroid was measured using the Wallac gamma counter.

3.3.3. Cell Distribution in 2D/3D Tumor Models

In U87 monolayer (2D) cell model, first, a centrifuge filter tube was used to achieve the final fluorescein isothiocyanate (FITC)

labeled samples with a polymer concentration of 3.48 mg mL⁻¹. Then, 20 µL of the FITC-labeled micelles were added to each dish and incubated for 30 min and 24 h. The control sample was prepared by adding 20 µL of PBS. The reaction was terminated by removing the suspension and washing the cell with PBS three times. To stain the lysosomes, 250 µL of 50 × 10⁻⁹ M LysoTracker Red (in PBS with pH value 7.4) was added to each dish and incubated for 45 min, which was followed by removing the LysoTracker Red solution and fixing the cells with 3.7% paraformaldehyde (PFA) solution for 15 min at room temperature. Next, we removed the cell fixation solution and added 2 mL of PBS to each dish. DAPI solution was added to each dish to stain the nucleus before confocal imaging. The confocal microscope used was a Nikon A1R confocal. Laser excitation at 405, 488, and 560 nm were applied for DAPI, FITC, and LysoTracker Red, respectively. The obtained data was analyzed with ImageJ software.

In U87 spheroid cell model, the diffusion of the PCL-PEO micelles (PCL-6500) within the tumor spheroids was followed by light-sheet fluorescence microscopy (LSFM) using a custom scanned Bessel-beam microscope with a 20×/NA1.0 objective (Olympus, XLUMPLFLN). Volumetric scans were obtained by scanning the excitation sheet with a pair of galvanometer mirrors while maintaining a focused image on the sCMOS camera (Andor, Zyla 4.2) with an electrically tunable lens (Optotune, EL-16-40-TC-VIS-20D). Two channels were imaged sequentially using excitation lasers at 488 nm (Coherent OBIS-488-LS, 1 mW) and 561 nm (Coherent OBIS-561, 1 mW) with bandpass emission filters with 525/39 nm and 620/52 nm (Thorlabs), respectively. To prepare samples, 0.2 mL of the obtained FITC-labeled micelles solution (polymer concentration: 3.48 mg mL⁻¹) was mixed with 1.5 mL of culture medium resulting in a solution with polymer concentration of 0.41 mg mL⁻¹. Then, 150 µL of the obtained samples was added to each spheroid (6 day culture) and incubated for 30 min and 24 h. Prior to imaging, spheroids were washed with PBS (twice) and stained with plasma membrane marker for 20 min. Then, intact spheroids were mounted in 2% low-melting temperature agarose inside a plastic capillary (FEP, Bola, S2022-04, inner diameter 0.8 mm) for imaging. The distribution of the micelles within the spheroids was followed using the FITC, whereas the membrane dye outlined each cell within the spheroid. Images were processed by Richardson-Lucy deconvolution using the ImageJ plug-in DeconvolutionLab2.^[21] and experimental point-spread functions measured with 500-nm fluorescent beads (Tetraspeck Microspheres).

3.3.4. Cell Growth Inhibition

The cell growth inhibition caused by the empty micelles, PTX-loaded micelles, ¹⁷⁷Lu-loaded micelles, and ¹⁷⁷Lu&PTX co-loaded micelles was first checked. Briefly, centrifuge filters were applied to exchange the solvent of the obtained micelles samples from HEPES buffer to PBS (pH 7.4). Then 20 µL of the sample solution was added to each U87 spheroid. After 1 day of incubation, the old culture medium was removed carefully, the spheroid was washed with PBS three times followed by adding 200 µL of fresh culture medium. The size of the spheroids was recorded at different timepoints using a binocular microscope. ImageJ software was used to analyze the obtained graphs.

3.3.5. CellTiter-Glo 3D Cell Viability Assays

CellTiter-Glo 3D Cell Viability Assay (ATP-based viability assay) was performed to determine the therapeutic effect of the micelles loaded with different anticancer substances. The drug administration process was exactly the same as that in the evaluation of cell growth inhibition. Rather than recording the morphology at different timepoints, the spheroids were sacrificed at Day 1 and Day 5 in order to determine the cell viability. For this purpose, all of the medium was carefully removed from the spheroid containing wells, then 200 μ L of a mixture composed by CellTiter-Glo 3D reagent and culture medium with a volume ratio of 1:1 was added to each spheroid and reacted for around 1 h. The spheroid in each counting well would be destroyed during the reaction. Finally, the luminescence of each well was measured by a fluorescence spectrophotometer. The setup parameters of fluorescence spectrophotometer are as followed: Bio/chemiluminescence data mode; emission wavelength of 600 nm, emission slit of 20 nm, open emission filter, gate time of 200 ms.

$$\text{Cell viability} = \frac{\text{The luminescent intensity of each sample}}{\text{The luminescent intensity of the control group}} \times 100\% \quad (2)$$

3.4. Statistical Analysis

All data points referred to the mean \pm standard deviation (SD) and were based on at least three separate experiments ($n = 3$). Statistical analysis of cell viability was accomplished by two-way analysis of variance (ANOVA) using GraphPad Prism version 8.0 software. The pairwise comparison of cell viability was performed with Bonferroni's test. The α value was set to 0.05 and the levels of statistical significance are represented as * $p \leq 0.05$, ** $p \leq 0.01$, *** $p \leq 0.001$, and **** $p \leq 0.0001$.

4. Results and Analysis

4.1. Formation of PTX-Loaded PCL-PEO Micelles

We applied PTX, a typical terpenoid drug, in this work as the chemotherapeutic agent.^[22,23] The PTX-loaded micelles were prepared by adding PTX during the self-assembly process of the block copolymer. According to previous publications, the presence of PTX may alter the morphology of the micelles.^[24,25] Therefore, we applied cryo-EM to observe the morphology of the PTX-loaded micelles obtained at different PTX/polymer mass ratios. The results in **Figure 1** show that rod-like structures were formed at a drug/polymer mass ratio of 2:20 with lengths up to several micrometers which were assumed to be PTX crystals.^[26] No micelles could be observed by cryo-EM. As we decreased the drug to polymer ratio to 1:20, some micelles (red arrows) appeared but long rods were still present. By further decreasing the drug amount to a mass ratio of 0.75:20, the rod-like structures disappeared, but instead some dense clusters (yellow arrows) were observed which were most likely composed of PTX. Only at a PTX:polymer mass ratio of 0.5:20, no PTX crystals could be detected indicating that the majority of PTX molecules were encapsulated in the micelles.

Therefore, we chose the drug:polymer mass ratio of 0.5:20 for further experiments. Two block-copolymers, i.e., PCL-PEO 2800-2000 and PCL-PEO 6500-5500 were used to encapsulate PTX. The PTX loading efficiency was $86.4 \pm 6.3\%$ and $75.7 \pm 6.8\%$ for PCL-PEO 2800-2000 (PTX-2800) and PCL-PEO 6500-5500 (PTX-6500), respectively. The DLS results in **Figure S1** (Supporting Information) show that the PTX-6500 micelles have a mean hydrodynamic radius of ≈ 50 nm and the PTX-2800 micelles have a radius of ≈ 16 nm. Although both polymers had comparable drug loading, in our previous experiment (**Figure S2**, Supporting Information), the radiolabeling stability of the ^{111}In & PTX co-loaded PCL-6500 micelles was better at lower pH, saying 5.2, which might occur in cells and therefore we choose to focus on polymer PCL-PEO 6500-5500.

4.2. Cell Uptake and Cellular Distribution of the Micelles Evaluated in 2D and 3D Cell Models

We first determined the intracellular distribution of PCL-6500 micelles using a 2D model of U87 (glioblastoma) tumor cells with confocal laser scanning microscopy (CLSM). For tracing the micelles, FITC-labeled PCL-6500 micelles were prepared. To determine the localization of the micelles in the cell, we stained the nuclei of the U87 cells with DAPI, and stained the lysosomes with LysoTracker Red. As shown in **Figure 2**, the uptake of the PCL-6500 was time-dependent, i.e., the green fluorescence signal from the FITC was very weak after 30 min of incubation but became more pronounced after 24 h, indicating that more micelles appeared inside the tumor cells. The merged images indicate that the PCL-6500 micelles mainly accumulated at the lysosomes, which might be due to the clathrin-mediated endocytosis process as observed for other polymeric nanocarriers.^[27–29]

We used a 3D tumor model composed of the same cells (U87) to further study the uptake and distribution of the micelles. The tumor spheroid contains a proliferation zone, a quiescence zone and a necrosis zone which mimics the complexity of in vivo tumors replicating vital characteristics of the tumor microenvironment.^[30] The amount of PCL-PEO micelles taken up by the U87 spheroids was evaluated using micelles radiolabeled with ^{111}In (III). **Figure 3a** shows that the spheroid uptake was found to be $0.19 \pm 0.06\%$ and $0.21 \pm 0.08\%$ for PCL-2800 and PCL-6500 micelles after 24 h of incubation, which increased to $2.20 \pm 0.44\%$ and $1.45 \pm 0.23\%$ after 72 h.

All further experiments were carried out with PCL-6500 which appeared to have better radiolabeling stability at lower pH (5.2) than then PCL-2800 (**Figure S2**, Supporting Information).

To further analyze the distribution of the PCL-6500 micelles within the 3D spheroid, we labeled them with FITC and used LSFM to visualize the micelles distribution in the intact spheroid. The main advantage of LSFM is that it enables imaging of the nanoparticle distribution in a 3D tumor model without prior need for tissue sectioning. **Figure 3b,c** is a visual representation of the penetrating capabilities of micelles in U87 multicellular tumor spheroids, at different time points. The distribution of the micelles within the spheroids was observed using FITC (green channel), whereas the membrane dye (magenta) outlined each cell within the spheroid. Spheroids were incubated with FITC-labeled micelles for 30 min or 24 h. **Figure 3d,g** shows that an in-

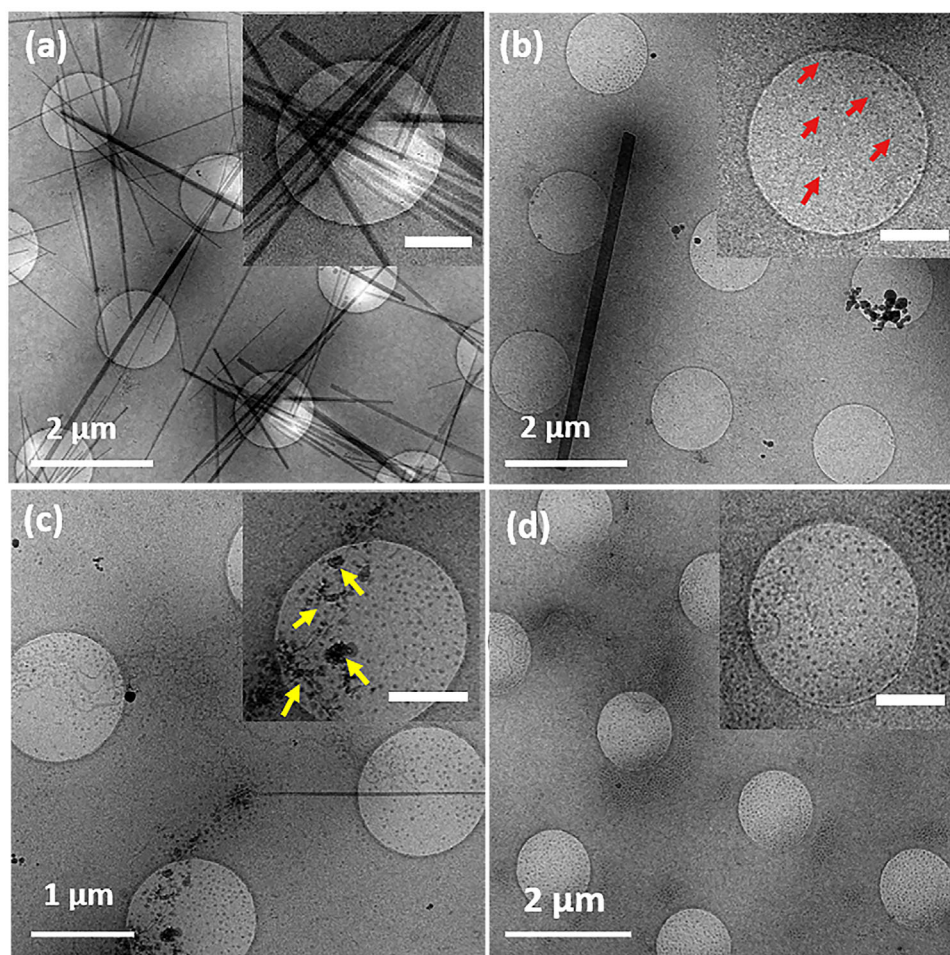


Figure 1. Cryogenic electron microscope (Cryo-EM) images of paclitaxel 2800 (PTX-2800) micelles prepared at PTX to polymer mass ratio of a) 2:20; b) 1:20; c) 0.75:20, and d) 0.5:20. Polymer concentration: 8.7 mg mL^{-1} , without filtration process, the scale bar in the zoom-in pictures represents 500 nm.

crease in incubation time of the micelles severely alters the distribution of the FITC-labeled micelles in the spheroid. At both time points, the structure of the cells composing the spheroid can be recognized by the membrane labeling in magenta (Figure 3e,h). Figure 3d depicts the fluorescence signal of the micelles which were incubated for 30 min. The signal from these micelles is diffuse and similarly distributed to the signal detected from the cell membranes (Figure 3e). The fluorescence distribution pattern indicates that after 30 min of incubation time the micelles were capable of penetrating inside the spheroid, but were not concentrated inside the cells. This is also supported by the overlap image (Figure 3f) where both the magenta and green color seem to outline the cell membrane. The brightest spots of the green fluorescent channel represent the locations where the micelles aggregated, since single micelles cannot produce high pixel intensities. Some clumps of saturated pixels in the red channel were also observed, attributed to aggregates of the cell membrane marker, which could be also observed in the spheroid only treated with membrane dye (Figure S3, Supporting Information).

After 24 h of incubation (Figure 3g) the green signal is 10-fold higher (under the same imaging conditions), indicating that more micelles are present. The distribution of the green signal

is also less diffuse than at 30 min incubation, and appears clustered in a large fraction of cells. These observations suggest that the majority of the micelles have passed through the cell membrane and accumulate inside the cells. The merged frames of Figure 3f,i support these observations, as in the 30 min group, both the green and red fluorescence overlap, revealing cell membranes and the cell arrangement within the spheroid. In contrast, for the 24 h group, the red fluorescence from the cell membrane is spatially distinct from the green signal, confirming the uptake of micelles in the cells. Videos S1, S2 (Supporting Information) show a z-stack revealing the micelle distribution throughout the spheroid, which show that increasing micelles have penetrated inside the spheroid and even entered the cells with prolonged incubation time.

4.3. Cell Killing Efficiency

We first used PTX-6500 micelles prepared with a PTX:polymer mass ratio of 0.5:20 to evaluate the influence of the drug alone on the growth of the U87 spheroids. The applied PTX-loaded micelles appeared to be very toxic to the tumor cells, and the

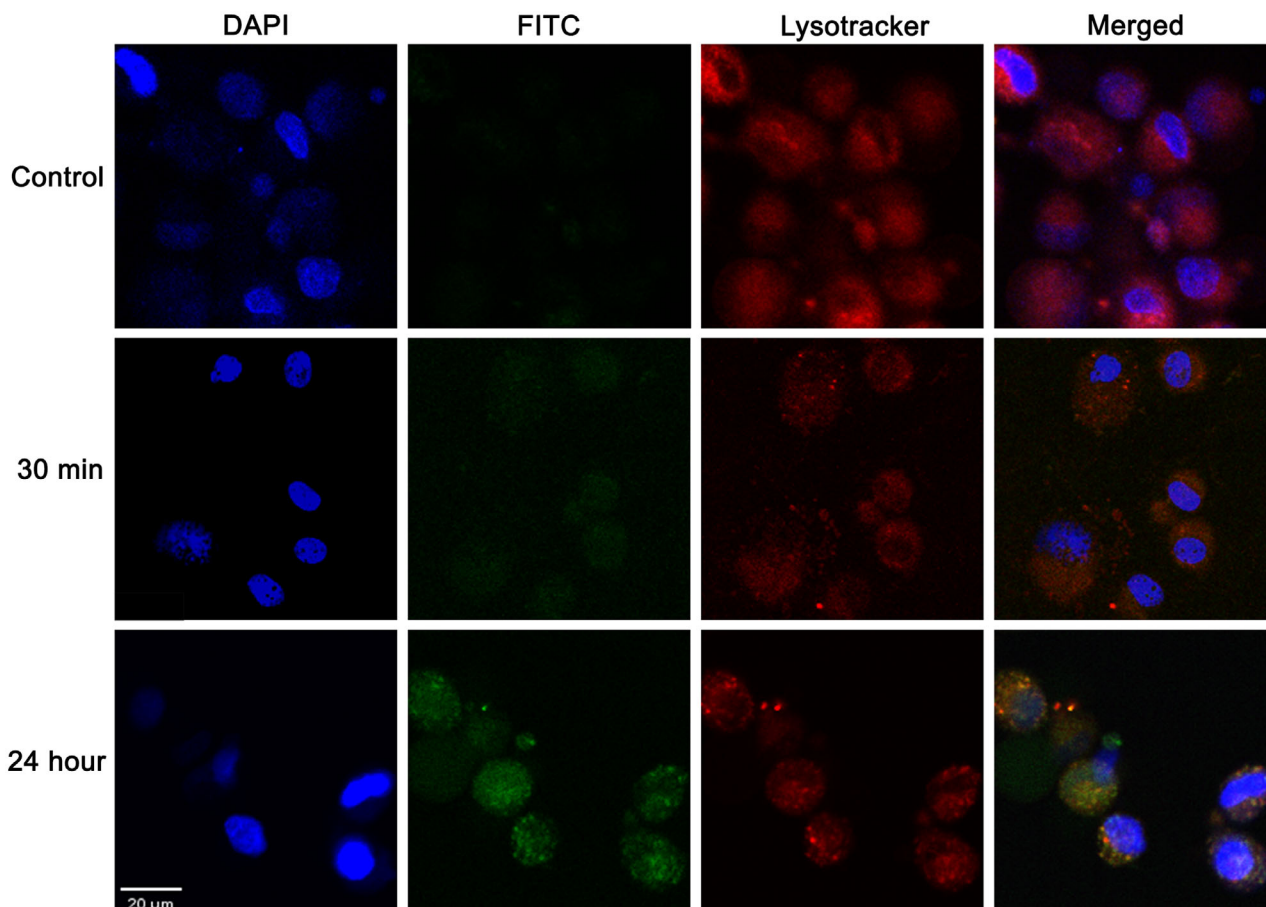


Figure 2. Intracellular distribution of fluorescein isothiocyanate (FITC) labeled PCL-6500 micelles in U87 cells imaged by a confocal laser scanning microscopy (CLSM) after incubation time of 30 min and 24 h. The control group had no micelles and contained only 20 μL of phosphate buffered saline (PBS) in addition to the cell culture. For the cells incubated with micelles, the polymer concentration was 0.26 mg mL^{-1} , nuclei were stained with DAPI, lysosomes were stained with Lysotracker Red.

spheroids displayed an evident shrinkage (the results are not shown in this work). Therefore, we decreased the encapsulated amount of PTX by preparing PTX-6500 micelles with a PTX:polymer mass ratio of 0.05/20 (marked as PTX-con-1X, X denotes the degree of dilution). To explore the influence of drug dosage on the tumor growth, we also prepared PTX-con-5X, PTX-con-10X, and PTX-con-20X by diluting a PTX-con-1X sample 5, 10, and 20 times.

The images of the spheroids treated with PTX-micelles are shown in Figure S3 (Supporting Information) together with empty micelles and PBS serving as the controls. The results indicate that the spheroids treated with drugs are characterized by a smaller size on Day 5 compared to the ones incubated with micelles and PBS. The spheroid growth tendency is summarized in Figure 4 and shows that the micelles themselves had an influence on tumor growth that is comparable to the PBS control group, indicating that the micelles themselves are not toxic to the tumor cells. Contrarily, the spheroids treated with PTX-loaded micelles showed evident shrinkage. As summarized in Figure 4a, no noticeable difference could be seen on day 0 (24 h after drug administration). On Day 1, all spheroids treated with drugs had clearly smaller sizes than those of the control group.

The influence of different PTX doses was evident from Day 2 onwards, where spheroids treated with the highest concentration ($3.6 \mu\text{g mL}^{-1}$) were much smaller than the ones treated with lower amounts of PTX (Figure S4, Supporting Information). On Day 5 the spheroids treated with the highest PTX concentration already showed evident shrinkage, while the spheroid size gradually increased with lower doses of PTX although at much lower rate than the control group.

Subsequently, we investigated the influence of the activity of $^{177}\text{Lu(III)}$ on the growth of the spheroids. For this purpose, three samples with different activities, denoted as M-0.06 MBq (activity given to each spheroid), M-0.15 MBq, and M-0.6 MBq were prepared. Figure 4b shows the results of the radionuclide treatment suggesting no evident size difference on Day 0, similar to the PTX experiments. The spheroids treated with $^{177}\text{Lu(III)}$ had much smaller size than the control group on Day 5 and the ones given 0.6 MBq even started to visibly fall apart (Figure S5, Supporting Information).

The combined radionuclide and chemotherapy treatment was carried out using ^{177}Lu &PTX co-loaded PCL-6500 micelles. To properly evaluate the therapeutic effects of the combined therapy, five samples were prepared, namely PTX-M, Lu-M,

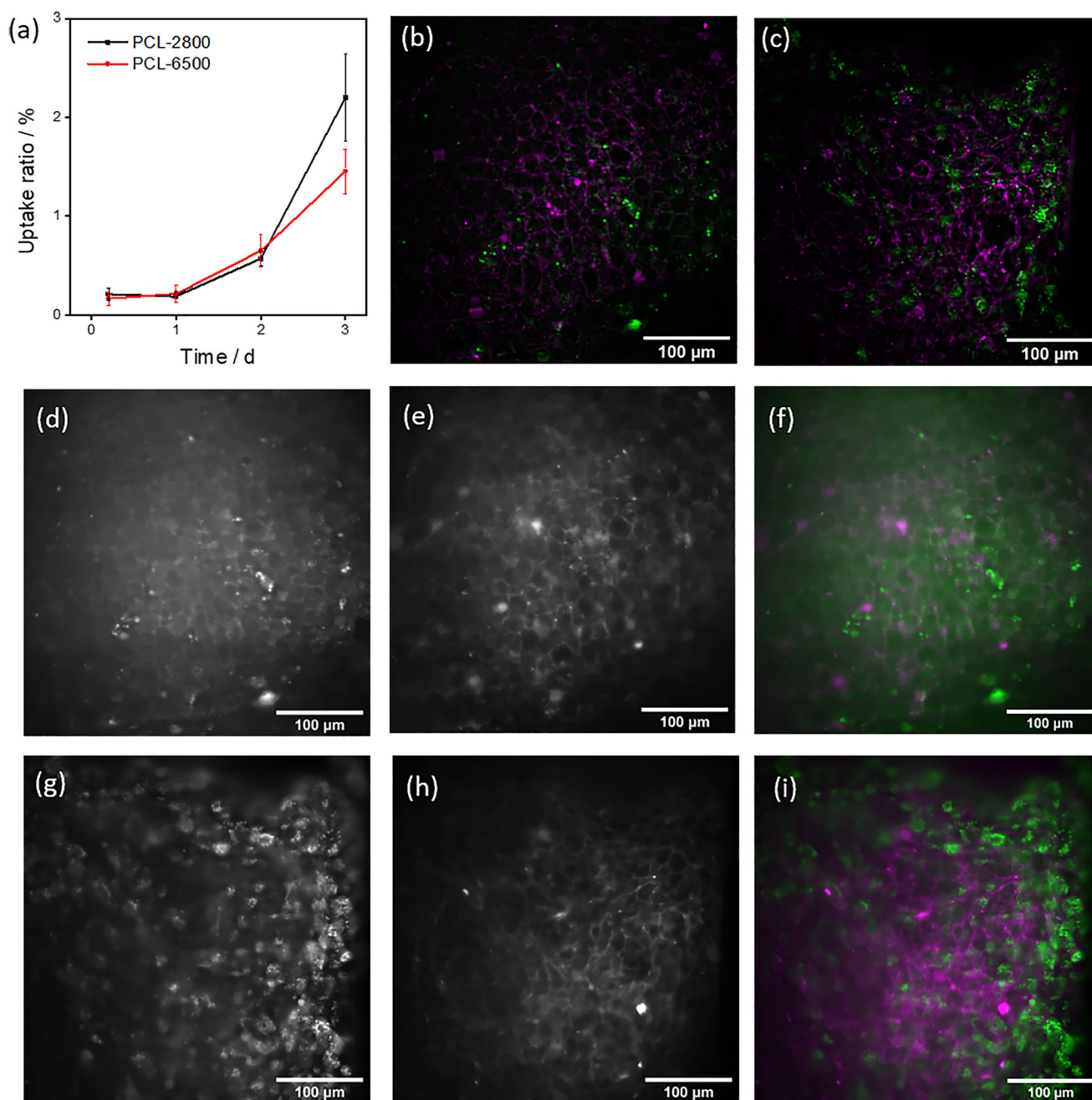


Figure 3. The uptake and distribution of the polymer micelles as function of time. d–i) Uptake of the PCL-6500 micelles. a) Spheroid uptake of ^{111}In -radiolabeled micelles as a function of time. Polymer concentration in the tumor uptake study was 0.079 mg mL^{-1} , the error bar represents the experimental uncertainty of $n = 4$. Deconvolved single-plane light-sheet fluorescence microscopy (LSFM) images of a spheroid after b) 30 min and c) 24 h incubation with fluorescein isothiocyanate (FITC) labeled micelles, the green color corresponds to the micelles, while the magenta color shows the cell membrane. For (d)–(i), showing images without deconvolution, the first column (d,g) depicts the green fluorescence signal emitted from the FITC-labeled micelles, while the second column (e,h) displays red fluorescence signal of the magenta membrane dye, which binds to the cell membranes within the spheroid. The final column (f,i) is an overlay of the two channels. The rows were sorted based on the incubation time, (d–f) corresponds to 30 min incubation whereas (g–i) corresponds to 24 h incubation. The polymer concentration in the light sheet imaging experiments was 0.41 mg mL^{-1} .

P&Lu-1X, P&Lu-2X, and P&Lu-5X. Among them, PTX-M and Lu-M denoted the single treatment with PTX and $^{177}\text{Lu(III)}$, respectively, the former had the same PTX concentration as P&Lu-1X with a PTX concentration of $0.48 \mu\text{g mL}^{-1}$, while the latter had the same activity as P&Lu-1X, i.e., 30 kBq of $^{177}\text{Lu(III)}$.

The P&Lu-2X and P&Lu-5X samples were two and five times dilutions of the P&Lu-1X samples, respectively.

As shown in **Figure 5a**, the single treatment with PTX and $^{177}\text{Lu(III)}$ could inhibit the spheroid growth, although the Lu-M with 30 kBq of $^{177}\text{Lu(III)}$ given to each spheroid showed lower

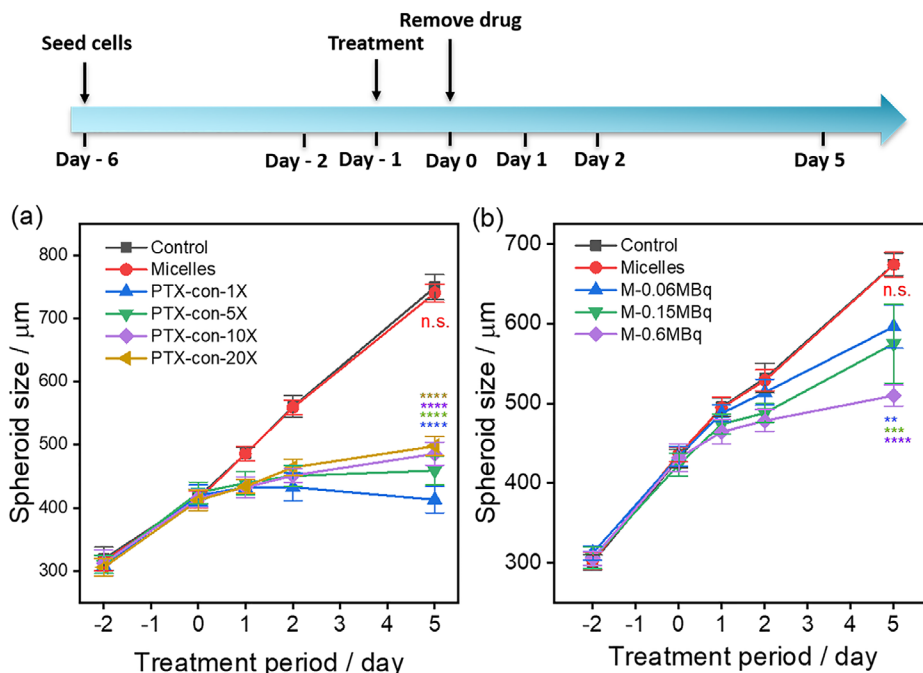


Figure 4. a) The size of spheroids when exposed to different paclitaxel (PTX) concentrations as function of time. Control: treated with 20 μL of phosphate buffered saline (PBS); Micelles: polymer concentration 1.58 mg mL^{-1} ; PTX-con-1X: polymer concentration 1.58 mg mL^{-1} , drug concentration 3.6 $\mu\text{g mL}^{-1}$; PTX-con-5X: polymer concentration 0.32 mg mL^{-1} , drug concentration 0.7 $\mu\text{g mL}^{-1}$; PTX-con-10X: polymer concentration 0.16 mg mL^{-1} , drug concentration 0.36 $\mu\text{g mL}^{-1}$. PTX-con-20X: polymer concentration 0.08 mg mL^{-1} , drug concentration 0.18 $\mu\text{g mL}^{-1}$. b) The size of the spheroid as function of time at different activities of $^{177}\text{Lu(III)}$. Control: no micelles just 20 μL of PBS added; Micelles: polymer concentration 1.32 mg mL^{-1} ; M-0.06MBq: polymer concentration 0.132 mg mL^{-1} and 0.06 MBq per spheroid; M-0.15 MBq: polymer concentration 0.33 mg mL^{-1} and 0.15 MBq per spheroid; M-0.6 MBq: polymer concentration 1.32 mg mL^{-1} and 0.6 MBq per spheroid. The error bar represents the experimental uncertainty of $n = 5$, * $p < 0.05$, ** $p < 0.01$, *** $p < 0.001$, **** $p < 0.0001$.

growth inhibition than the PTX-M sample with a PTX concentration of 0.48 $\mu\text{g mL}^{-1}$. The combined therapy already showed its potential on the second day after drug and radionuclide administration resulting in an evidently slower spheroid growth than both the control group and the spheroids receiving single treatment. Typical images of the spheroids treated in this study can be seen in Figure 5a. The spheroid of the control group continued to grow during the whole observation period and had a smooth surface on Day 5. Although the spheroids that received single treatment had a smaller size on Day 5 compared to the control group, their surface still remained smooth, while the combined treatment, even a low drug concentration of 0.096 $\mu\text{g mL}^{-1}$ and a low radiation dose of 6 kBq, clearly led to fuzzy spheroid surface, indicating the start of disintegration.

The fuzzy spheroid surface made it difficult to determine the size of the spheroid in a precise way. Therefore, an ATP test was carried out to evaluate the viability of the spheroids when exposed to the different treatments. The viability on Day 0 and Day 5 was measured and shown in Figure S5 (Supporting Information) and Figure 5c. The single treatment with PTX or $^{177}\text{Lu(III)}$ did not appear to be toxic on Day 0 with similar viability as the control group. However, the PTX treatment showed higher toxicity on Day 5, with only 80.5 \pm 10.6% of the cells being alive. The $^{177}\text{Lu(III)}$ treated spheroid had viability on Day 5 of nearly 100% when compared to the control group, indicating that 30 kBq of $^{177}\text{Lu(III)}$ was insufficient to cause cell damage under these experimental conditions.

In terms of the combined treatment, an interesting phenomenon occurred, that is, the addition of P&Lu-2X and P&Lu-5X with low dose of both PTX and $^{177}\text{Lu(III)}$ initially led to better growth of the spheroid on Day 0 (more viable cells than the control group, Figure S6, Supporting Information). This phenomenon may be related to low drug dose activating certain growth-related factors found in tumors.^[31] On Day 5, the combined treatment samples lead to 57.4 \pm 1.3, 63.2 \pm 2.6, and 51.6 \pm 13.1% viability for P&Lu-1X, P&Lu-2X, and P&Lu-5X, respectively, which is much better than the single treatment with a viability of 80.5 \pm 10.5% and 101.4 \pm 10.8% for chemotherapy and radionuclide therapy, indicating that the combined treatment was more efficient. However, the viability test of the co-loaded micelles did not show dose-dependent behavior, which may be due to the limited penetration depth in the spheroid. It is possible that the combined treatment mainly affects the cells in the proliferation zone within the chosen treatment time (5 days). Moreover, we also checked the viability of the cells treated with empty micelles which confirmed that the nanocarriers were not toxic to the U87 cells and had a comparable number of living cells as the PBS control group on both Day 0 and Day 5.

5. Conclusion

The work in this paper aimed to analyze the potential of combined radionuclide and chemotherapy in the treatment of cancer. We systematically carried out in vitro experiments to evaluate the

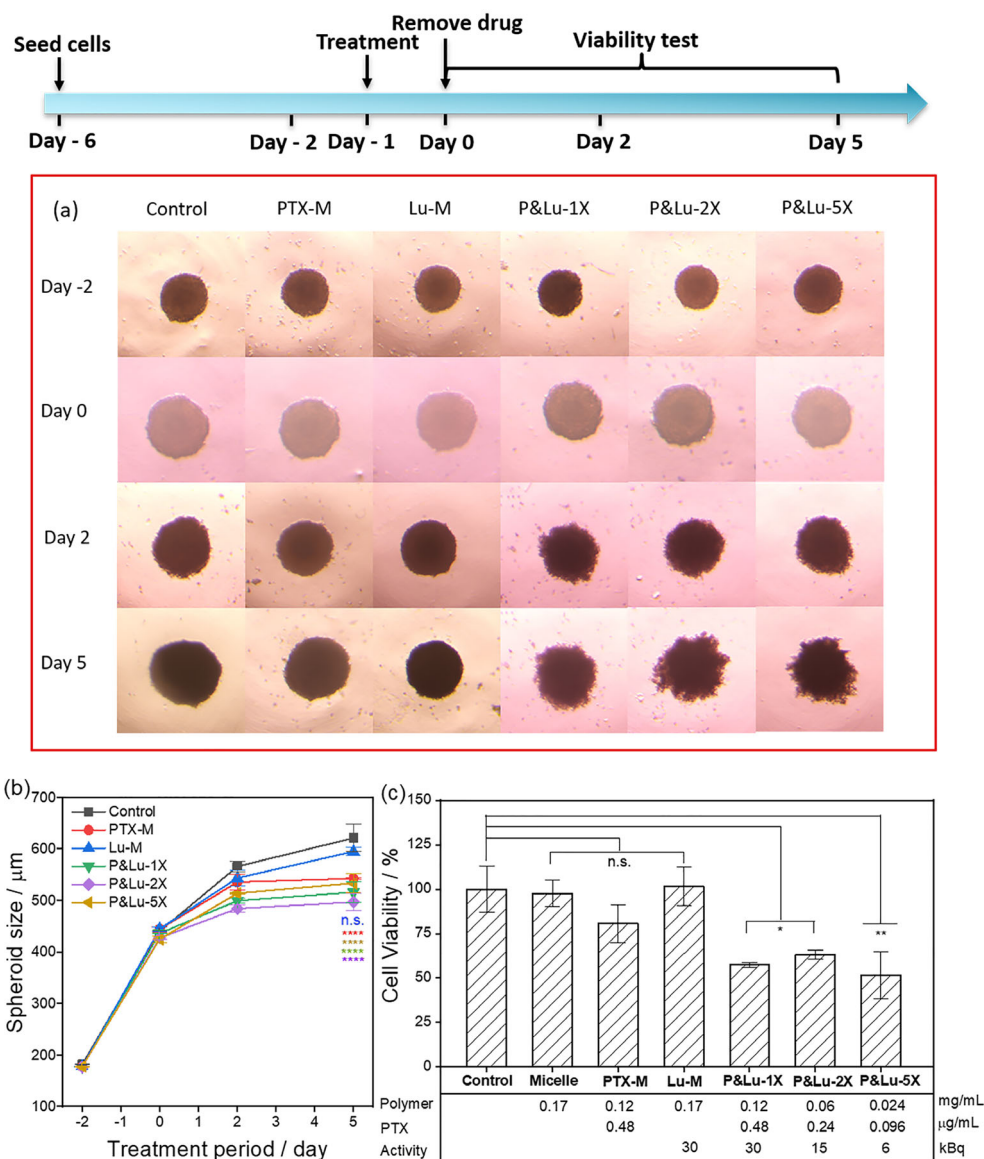


Figure 5. a) Representative images of the spheroids for the various treatments and at different time points. b) The size of the spheroids exposed to paclitaxel (PTX) or ^{177}Lu (III) loaded micelles and PTX and ^{177}Lu co-loaded micelles as a function time. c) Percentage of viable cells on Day 5 of the spheroids when exposed to the different treatments. Control: no micelles just 20 μL of phosphate buffered saline (PBS) added Micelles: polymer concentration 0.17 mg mL^{-1} . PTX-M: polymer concentration 0.12 mg mL^{-1} , PTX concentration 0.48 $\mu\text{g mL}^{-1}$; Lu-M: polymer concentration 0.17 mg mL^{-1} , 30kBq of ^{177}Lu (III); P&Lu-1X: polymer concentration 0.12 mg mL^{-1} , PTX concentration 0.48 $\mu\text{g mL}^{-1}$, 30kBq of ^{177}Lu (III); P&Lu-2X: polymer concentration 0.06 mg mL^{-1} , PTX concentration 0.24 $\mu\text{g mL}^{-1}$, 15 kBq of ^{177}Lu (III); P&Lu-5X: polymer concentration 0.024 mg mL^{-1} , PTX concentration 0.096 $\mu\text{g mL}^{-1}$, 6 kBq of ^{177}Lu (III). The error bars represent the experimental uncertainty of $n = 3$. * $p < 0.05$, ** $p < 0.01$, *** $p < 0.001$, **** $p < 0.0001$.

effect of PCL-PEO micelles having different cargos. 2D cell studies showed that the micelles accumulate in or around the lysosomes of the cells as expected, while 3D cell studies demonstrated that the micelles were able to diffuse into the spheroids within 24 h. Subsequently, we used PTX-loaded micelles, ^{177}Lu (III) radio-labeled micelles, and PTX + ^{177}Lu co-loaded micelles to evaluate their therapeutic efficiency using growth retardation studies combined with a viability assay in 3D cell models. The growth evaluation revealed that the combined treatment was the most effective and this was further confirmed by the viability tests. The results showed that at low activity of ^{177}Lu (III) combined with low

amounts of PTX, high killing efficiency could be obtained, which is beneficial in reducing side effects caused by the chemotherapeutic drugs to healthy tissue. Nevertheless, more studies need to be conducted to further explore the mechanism and treatment optimization of this combination treatment strategy.

Supporting Information

Supporting Information is available from the Wiley Online Library or from the author.

Acknowledgements

This work is financially supported by the China Scholarship Council (Grant Number 201707040083) and the Delft Health Initiative. E.C. acknowledges support from an ENW-XS grant (OCENW.XS.102) from the Dutch Research Council (NWO). We are grateful to Erik de Blois from Erasmus MC for the supply of ¹⁷⁷Lu, we also thank Rene Nouse for the radioisotope transportation. We would also like to thank Laura Maddalena and Dr. Nicolò Ceffa for help with the light-sheet fluorescence microscope and preliminary light-sheet studies.

Conflict of Interest

The authors declare no conflict of interest.

Author Contributions

H.L. performed the majority of experiments and data analysis and drafted the manuscript. R.A.N. worked on 3D cell staining and supported the light sheet imaging. R.P.F. mainly work on the confocal laser scanning microscopy. A.C.L. helped with the Cryo-EM pictures. B.D. and A.v.d.M. helped with the 3D cell growing and viability tests. R.W. helped with statistical analysis. Q.v.C. conducted the light-sheet imaging tests and E.C. helped to analyze the data. R.E. and A.G.D. guided the experimental process, analyzed the data, and revised the manuscript.

Data Availability Statement

The data that support the findings of this study are available from the corresponding author upon reasonable request.

Keywords

biodistribution, cell viability, chemoradionuclide therapy, polymeric micelles, tumor spheroid

Received: September 15, 2022

Revised: February 10, 2023

Published online:

- [1] M. Zak, J. Drobniak, *Strahlentherapie* **1971**, 142, 112.
- [2] S. Nagasawa, J. Takahashi, G. Suzuki, Y. Hideya, K. Yamada, *Int. J. Mol. Sci.* **2021**, 22, 3140.
- [3] E. B. Golden, S. C. Formenti, P. B. Schiff, *Anticancer Drugs* **2014**, 25, 502.
- [4] X. Yi, L. Chen, J. Chen, D. Maiti, Z. Chai, Z. Liu, K. Yang, *Adv. Funct. Mater.* **2018**, 28, 1705161.
- [5] G. D. Wilson, S. M. Bentzen, P. M. Harari, *Semin. Radiat. Oncol.* **2006**, 16, 2.
- [6] M. Zwitter, V. Kovac, U. Smrdel, P. Strojjan, *J. Thorac. Oncol.* **2006**, 1, 662.
- [7] S. Kranjc Brezar, A. Prevc, M. Niksic Zakelj, A. Brozic, M. Cemazar, P. Strojjan, G. Sersa, *Sci. Rep.* **2020**, 10, 1563.
- [8] K. Mortezaee, A. Narmani, M. Salehi, H. Bagheri, B. Farhood, H. Haghi-Aminjan, M. Najafi, *Life Sci.* **2021**, 269, 119020.
- [9] A. Herskovic, K. Martz, M. al-Sarraf, L. Leichman, J. Brindle, V. Vaitkevicius, J. Cooper, R. Byhardt, L. Davis, B. Emami, *N. Engl. J. Med.* **1992**, 326, 1593.
- [10] L. Tian, Q. Chen, X. Yi, G. Wang, J. Chen, P. Ning, K. Yang, Z. Liu, *Theranostics* **2017**, 7, 614.
- [11] X. Zhong, K. Yang, Z. Dong, X. Yi, Y. Wang, C. Ge, Y. Zhao, Z. Liu, *Adv. Funct. Mater.* **2015**, 25, 7327.
- [12] K. Liu, D. Zheng, J. Zhao, Y. Tao, Y. Wang, J. He, J. Lei, X. Xi, *J. Mater. Chem. B* **2018**, 6, 4738.
- [13] A. Yordanova, H. Ahrens, G. Feldmann, P. Brossart, F. C. Gaertner, C. Fottner, M. M. Weber, H. Ahmadzadehfar, M. Schreckenberger, M. Miederer, M. Essler, *Clin. Nucl. Med.* **2019**, 44, e329.
- [14] A. G. Denkova, H. Liu, Y. Men, R. Eelkema, *Adv. Ther.* **2020**, 3, 1900177.
- [15] P. Kumari, B. Ghosh, S. Biswas, *J. Drug Targeting* **2016**, 24, 179.
- [16] M. E. Werner, N. D. Cummings, M. Sethi, E. C. Wang, R. Sukumar, D. T. Moore, A. Z. Wang, *Int. J. Radiat. Oncol., Biol., Phys.* **2013**, 86, 463.
- [17] S. Gao, T. Li, Y. Guo, C. Sun, B. Xianyu, H. Xu, *Adv. Mater.* **2020**, 32, 1907568.
- [18] A. Z. Wang, K. Yuet, L. Zhang, F. X. Gu, M. Huynh-Le, A. F. Radovic-Moreno, P. W. Kantoff, N. H. Bander, R. Langer, O. C. Farokhzad, *Nanomedicine* **2010**, 5, 361.
- [19] P. Huang, Y. Zhang, W. Wang, J. Zhou, Y. Sun, J. Liu, D. Kong, J. Liu, A. Dong, *J. Controlled Release* **2015**, 220, 456.
- [20] H. Liu, A. C. Laan, J. Plomp, S. R. Parnell, Y. Men, R. M. Dalgliesh, R. Eelkema, A. G. Denkova, *ACS Appl. Polym. Mater.* **2020**, 3, 968.
- [21] D. Sage, L. Donati, F. Soulez, D. Fortun, G. Schmit, A. Seitz, R. Guiet, C. Vonesch, M. Unser, *Methods* **2017**, 115, 28.
- [22] M. Shahin, A. Lavasanifar, *Int. J. Pharm.* **2010**, 389, 213.
- [23] E. K. Rowinsky, R. C. Donehower, *N. Engl. J. Med.* **1995**, 332, 1004.
- [24] A. Schulz, S. Jaksch, R. Schubel, E. Wegener, Z. Di, Y. Han, A. Meister, J. Kressler, A. V. Kabanov, R. Luxenhofer, C. M. Papadakis, R. Jordan, *ACS Nano* **2014**, 8, 2686.
- [25] C. Cao, J. Zhao, F. Chen, M. Lu, Y. Y. Khine, A. Macmillan, C. J. Garvey, M. H. Stenzel, *Chem. Mater.* **2018**, 30, 5227.
- [26] S. Farah, A. J. Domb, *J. Controlled Release* **2018**, 271, 107.
- [27] L. M. Bareford, P. W. Swaan, *Adv. Drug Delivery Rev.* **2007**, 59, 748.
- [28] L. Xu, Y. Yang, M. Zhao, W. Gao, H. Zhang, S. Li, B. He, Y. Pu, *J. Mater. Chem. B* **2018**, 6, 1076.
- [29] Z. Zhang, X. Xiong, J. Wan, L. Xiao, L. Gan, Y. Feng, H. Xu, X. Yang, *Biomaterials* **2012**, 33, 7233.
- [30] M. P. Carvalho, E. C. Costa, S. P. Miguel, I. J. Correia, *Carbohydr. Polym.* **2016**, 150, 139.
- [31] B. Liu, S. Pan, X. Dong, H. Qiao, H. Jiang, G. W. Krissansen, X. Sun, *Cancer Sci.* **2006**, 97, 675.